Journal of Applied Physics

Advanced polymer dielectrics for high temperature capacitive energy storage

Cite as: J. Appl. Phys. **127**, 240902 (2020); https://doi.org/10.1063/5.0009650
Submitted: 01 April 2020 • Accepted: 06 June 2020 • Published Online: 23 June 2020

Yao Zhou and Qing Wang

Journal of Applied Physics PERSPECTIVE scitation.org/journal/jap

Advanced polymer dielectrics for high temperature capacitive energy storage

Cite as: J. Appl. Phys. **127**, 240902 (2020); doi: 10.1063/5.0009650
Submitted: 1 April 2020 · Accepted: 6 June 2020 ·
Published Online: 23 June 2020

Yao Zhou and Qing Wang[a)]

AFFILIATIONS

Department of Materials Science and Engineering, The Pennsylvania State University, University Park, Pennsylvania 16802, USA

[a)]**Author to whom correspondence should be addressed:** wang@matse.psu.edu

ABSTRACT

Dielectric polymers are critical to meet the increasing demands for high-energy-density capacitors operating in harsh environments, such as aerospace power conditioning, underground oil and gas exploration, electrified transportation, and pulse power systems. In this perspective article, we present an overview of the recent progress in the field of polymer dielectrics for high temperature capacitive energy storage applications. Particular attention is placed on the underlying physical mechanisms of the rational design and the material structure–dielectric property–capacitive performance relationship. The scientific and technological challenges that remain to be addressed and the opportunities for future research are also presented.

I. INTRODUCTION

Dielectric materials are the basis of a fundamental electric circuit element, dielectric capacitor, which can be found in almost all electric circuits.[1–4] Dielectric capacitors are used to control and store electric charge and electrical energy in electrical and electronic devices,[5,6] such as electric power converters, pulse power systems, and electric power systems. For example, dielectric capacitors convert the DC electricity from sources such as batteries to AC electricity in the power inverters of hybrid electric vehicles (HVEs), in which motors are driven by AC power.[7] Compared with their ceramic counterparts, polymer dielectrics possess the intrinsic advantages of high breakdown strength, low energy loss, excellent mechanical flexibility, great reliability, low cost, and being lightweight, which make them an ideal material choice for high-energy-density capacitors.[8–12]

With the booming demands for capacitors with applications in various extreme conditions,[13] e.g., aerospace,[14] underground oil and gas exploration,[15] electrified transportation, and advanced electromagnetic systems,[16] there is an urgent need for dielectric capacitors capable of functioning efficiently under elevated temperatures and high electric fields. For example, the near-engine temperature in HVEs can reach above 140 °C. The utilization of wide bandgap semiconductors, e.g., silicon carbide (SiC) and gallium nitride (GaN), boosts the operation temperature of capacitors used in future power electronic devices beyond 150 °C.[15] However, the state-of-the-art biaxially oriented polypropylene (BOPP) film can only operate under 105 °C.[17] A secondary cooling system is thus required to accommodate the BOPP-based capacitors in the harsh-environment applications,[18] which unfortunately introduces extra volume, weight, and energy costs.[19–21] In some applications, the temperature requirement of capacitors is even more challenging, e.g., the operation temperature for capacitors used in underground oil and gas exploration and electrified aircrafts can exceed 200 °C and 250 °C, respectively, which makes the additional cooling system very costly or even impossible.

To meet the urgent demands of high-temperature high-energy-density capacitors, extensive research on high temperature polymer dielectrics has been conducted.[22–26] Typically, there are two main obstacles to the development of high temperature polymer dielectrics. One is the low thermal stability, and the other is the large conduction current under high temperatures and high electric fields. The thermal stability of polymer dielectrics is relatively low because of their low glass transition temperatures, which not only restricts the operation temperature of polymer dielectrics but also decreases the dielectric performance at high temperatures. A general strategy to improve the thermal stability of polymer dielectrics is to introduce rigid components in the structures, such as aromatic rings, heteroaromatic rings, hydrogen bonds, and high-strength chemical bonds. A variety of high thermal stability polymers have been exploited as high temperature polymer dielectrics, including polycarbonate (PC),

polyimide (PI), poly(ether imide) (PEI), poly(amide imide) (PAI), poly(benzimidazole) (PBI), poly(ethylene naphthalate) (PEN), poly (phenylene sulfide) (PPS), poly(ether ether ketone) (PEEK), poly (ether sulfone) (PESU), and fluorene polyester (FPE). Unfortunately, all the polymers show poor charge/discharge efficiencies under high temperatures and high electric fields, which is due to the sharply increased leakage current because of various temperature- and electric field-dependent electrical conduction mechanisms. Apart from the commercially available high temperature polymers, there are newly developed polymer materials that exhibit promising high temperature energy storage performance. For example, the crosslinked poly(arylene ether nitrile) film shows stable dielectric constant and low dielectric loss up to 300 °C.[27] The synthesized poly(phthalazinone ether ketone) film can deliver an energy density of 2 J/cm^3 even at the high temperature of 190 °C.[26] More recently, the polymer composites with ceramic nanofillers have been developed as a new class of high temperature polymer dielectrics. The main purpose of incorporating nanofillers into a polymer matrix is to suppress the high temperature leakage current so as to increase the charge/discharge efficiency and the discharged energy density. Nanofillers, especially nanofillers with high aspect ratio, can effectively improve the high temperature capacitive performance by the interfacial coupling and confinement effects. For example, boron nitride nanosheets (BNNSs) can effectively suppress the conduction current and increase the thermal conductivity of polymers. The crosslinked divinyltetramethyldisiloxane-bis(benzocyclobutene) (*c*-BCB)-based nanocomposites with BNNSs can deliver an energy density of 2 J/cm^3 at 200 °C. Even at 250 °C, where none of the high temperature polymers can function effectively, the *c*-BCB/BNNS nanocomposite can still deliver an energy density of 1.8 J/cm^3.[28] With the carefully designed nanostructure of the polymer nanocomposites, the delivered energy density can be boosted to 4.2 J/cm^3 at 150 °C.[29]

Although the field of high-temperature polymer dielectrics has witnessed exciting progress over the past several years, there exist significant challenges owing to the limited understanding of the underlying dielectric and conduction mechanisms of polymer dielectrics, especially under high electric fields and elevated temperatures. There are various challenges in the development of high temperature polymer dielectrics, including the development of the structure–property relationship, the rational design of the material and film structures, as well as the scalable production of the polymer dielectric films. Herein, we first summarize the fundamentals of the required properties for high-temperature polymer dielectrics. We then review the recent progress in high-temperature polymer dielectrics, together with the critical issues to be addressed. Finally, we highlight some challenges and opportunities for future development in this field.

II. CHARACTERISTIC PROPERTIES FOR HIGH TEMPERATURE DIELECTRICS

A. Dielectric constant and dissipation factor

For linear dielectrics (the electrical polarization scales linearly with the electric field), the stored energy density U_e scales linearly with the dielectric constant (ε_r) of the dielectric materials and also scales quadratically with the applied electric field, which can be expressed as[30]

$$U_e = \frac{1}{2}\varepsilon_r\varepsilon_0 E^2, \tag{1}$$

where ε_r is the dielectric constant of the dielectric material, ε_0 is the dielectric constant of vacuum, and E is the applied electric field. Since the stored energy density is proportional to the dielectric constant, the energy density of the capacitors can be increased by increasing the dielectric constant, which would reduce the volume and weight of the capacitors to meet the ever-increasing demand on highly integrated, compact, and miniaturized electronics and electric power systems.

Dielectric loss, which is also known as dissipation factor or loss tangent ($\tan\delta$), is a parameter that reflects the energy loss during the polarization-depolarization process of dielectric materials.[31] The dielectric loss not only decreases the discharged energy density and the charge/discharge efficiency of the capacitors, but also generates waste heat. Therefore, it is desired to concurrently increase the dielectric constant and decrease the dielectric loss. Since the polarization of dielectric materials depends on both temperature and frequency, the dielectric constant and dielectric loss both show temperature- and frequency-dependent characteristics. Therefore, weak dependence of dielectric properties on temperature and frequency is required for dielectric materials operating in a wide temperature and frequency range.

B. Dielectric breakdown strength and models

Dielectric breakdown strength (E_b) is the minimum electric field at which an insulator becomes a conductor. As shown in Eq. (1), the stored energy density scales quadratically with the applied electric field. The enhancement of the breakdown strength can substantially increase the stored energy density. For polymeric dielectric materials, there are mainly three breakdown mechanisms, i.e., electronic breakdown, thermal breakdown, and mechanical breakdown.[32–34]

The electronic breakdown in solid dielectrics is based on the collisional ionization.[32] A few conduction electrons would be accelerated by the applied electric field, and the resulting high speed electrons would impact the polymer chain and cause initial dielectric breakdown. Among the breakdown theories within the framework of electronic breakdown (i.e., intrinsic breakdown, electron avalanche breakdown, field emission breakdown, and free volume breakdown), free volume breakdown is the most common breakdown process in polymer dielectrics operating at high temperatures because the free volume would increase considerably when the temperature reaches the glass transition temperature (T_g) or melting temperature (T_m) of the polymer dielectrics.[35]

The thermal breakdown is the process associated with the heating and temperature increase in the dielectric materials due to electrical conduction and dielectric dissipation.[32] The increased temperature would further lower the electrical resistivity of the dielectric materials because of the temperature-dependent conduction mechanisms,[36] and thus increase the heat generation. When the heat generation exceeds the heat dissipation, the temperature of

the dielectric materials would continue to increase and cause thermal breakdown and thermal runway.[37]

The mechanical breakdown is the breakdown process associated with the mechanical deformation of the dielectric materials under applied electric fields.[32] The mechanical breakdown is usually observed in soft polymer dielectrics with limited technological significance, since the polymer dielectrics are usually not used above their softening temperatures.

C. Electrical conduction and mechanisms

The electrical conduction of polymer dielectrics is related to many factors, including the intrinsic material properties, applied electric field, and temperature. Under high electric fields and high temperatures, the conduction mechanism would change from linear Ohm's conduction into various nonlinear conduction mechanisms, including hopping conduction, Schottky emission, and Poole–Frenkel emission.[38–41] With the nonlinear conduction mechanisms, the leakage current increases sharply under high electric fields and high temperatures, which leads to continuous heat generation and temperature rise inside the dielectric materials. As a result, the working temperature and the breakdown field of film capacitors are often limited by electrical conductivity that increases sharply with the applied field and temperatures.

Hopping conduction usually occurs in the bulk of dielectric materials.[41] The semi-crystalline nature of polymer dielectrics denotes a short-range ordered but a long-range disordered structure. Therefore, the band structure only continues at the local ordered region, but discontinues between the different local ordered regions, which establishes a potential barrier between two ordered regions. The charge carriers can only jump between the ordered regions under thermal activation. Schottky emission is a kind of electrode-limited conduction processes, which is governed by the barrier height at the electrode/dielectric interface.[38] Under the presence of high temperatures and high electric fields, the charge carriers that overcome the potential barrier at the electrode/dielectric interface are injected into the dielectric materials to participate in the conduction process. Similar to Schottky emission, the presence of electric field can also decrease the barrier height of charge traps inside the dielectric material, thereby enabling more charge carriers to participate in the conduction process and increase the conduction current under high electric fields. This bulk-limited conduction process is the so-called Poole–Frenkel emission.[41]

For all the aforementioned conduction mechanisms, the increase in temperature can result in dramatically increased conduction current, thus significantly increasing the probability of thermal runaway. Therefore, the suppression of the conduction current is of critical importance for the polymer dielectrics operating at elevated temperatures and high electric fields.

D. Thermal stability and thermal conductivity

Thermal stability is a prerequisite for polymer dielectrics operating under high temperatures because high thermal stability ensures the material to have sufficient physical integrity. The glass transition temperature (T_g) of most polymer dielectrics is below 100 °C.[42] For amorphous polymer dielectrics, they would lose their mechanical toughness and undergo large changes in physical properties when the temperature is above their T_g, including the increase in dielectric constant, dielectric loss, and conduction current and the reduction in breakdown strength. For polymer dielectrics with high crystallinity, the melting temperature (T_m) instead of T_g is used to characterize the thermal stability because the crystal phase plays a dominate role in these materials. It should be noted that while high thermal stability is the prerequisite for high-temperature polymer dielectrics, the temperature-dependent electrical properties (e.g., conductivity, breakdown strength) must be taken into account to determine the operation temperature of a specific polymer dielectric. To increase the thermal stability (i.e., obtaining high T_g or T_m) of polymer dielectrics, there are usually three approaches, namely, (a) increasing the rigidity of the main chain by introducing rigid units; (b) incorporating bulky side groups to hinder the chain rotation; and (c) creating inter-chain chemical crosslinks to restrict the chain movement.

Another important thermal property for high-temperature polymer dielectric is the thermal conductivity (λ). Since thermal runaway plays an important role in the failure of film capacitors, increasing the thermal conductivity, which accelerates the heat dissipation, is beneficial to hinder the thermal runway. However, most polymer dielectrics are thermally insulated with low thermal conductivities in the range of 0.1–0.6 W/m K.[43] One approach to increase the thermal conductivity of polymer dielectrics is to introduce inorganic fillers with high thermal conductivities, but the drawback with this approach is that the electrical performance might be decreased.[44–46] It is essential to increase the thermal conductivity, while maintaining sufficient electrical insulation performance of dielectric materials.

III. ADVANCES IN HIGH TEMPERATURE POLYMER DIELECTRICS

A. High temperature polymers

Research on polymers for high temperature dielectric application is mostly concentrated on the improvement of thermal stability (e.g., high T_g) and dielectric properties (e.g., high dielectric constant). Table I summarizes the physical properties of representative high temperature polymer dielectrics. Considering the thermal and electrical properties of these polymer dielectrics, the most promising high temperature polymer dielectrics are PI, PEI, and FPE.

PI is a thermoset material synthesized by the polycondensation and imidization of dianhydride and diamine monomers.[47] One classical example of PI [Fig. 1(a)] is composed of pyromellitic dianhydride (PMDA) and 4,4′-oxydianiline (ODA). With the imide and aromatic structure in the main chain, PI possesses exceptionally high thermal resistance with a very high T_g of 360–410 °C, as well as excellent chemical resistance and decent mechanical strength.[48] At room temperature, PI exhibits a dielectric constant of 3.4 and a dissipation factor of 0.002. As conduction loss increases sharply under high temperatures and high electric fields, the charge/discharge efficiency of PI at 150 °C and an electric field of 300 MV/m is only 15%, which means that 85% of the stored energy becomes Joule heat, resulting a low discharged energy density of only 0.36 J/cm^3.[49] Such results confirm that even with outstanding thermal stability, the operation temperature of PI is

TABLE I. Properties of representative high temperature polymer dielectrics. PET, polyester; PEN, poly(ethylene naphthalate); PPS, poly(phenylene sulfide); PEEK, poly(ether ether ketone); PC, polycarbonate; PESU, poly(ether sulfone); PEI, poly (ether imide); FPE, fluorene polyester; PI, polyimide; c-BCB, crosslinked divinyltetramethyldisiloxane-bis(benzocyclobutene).

Dielectric	T_g (°C)	ε_r	tan δ	E_b (MV/m) (thickness)	λ (W/m K)
PET	75	3.3	0.005	300 (25 μm)	0.15
PEN	120	3.2	0.005	160 (75 μm)	0.15
PPS	120	3.2	0.002	490 (9 μm)	0.30
PEEK	150	3.1	0.004	200 (50 μm)	0.32
PC	150-210	3.2	0.002	500 (10 μm)	0.21
PESU	225	3.5	0.001	180 (25 μm)	0.18
PEI	217-260	3.2	0.001	200 (25 μm)	0.22
FPE	330	2.8-3.2	0.006	430 (8 μm)	0.20
PI	360-410	3.4-3.5	0.002	300 (25 μm)	0.12
c-BCB	>350	2.75	0.001	300 (10 μm)	0.30

actually limited by the electrical conduction under high temperatures and high electric fields. Therefore, it is more meaningful to suppress the electrical conductivity rather than simply increase T_g for high temperature polymer dielectrics.

PEI with an ether (–O–) linkage in its backbone is considered as a modified version of PI [Fig. 1(b)]. With the introduced ether linkage, the processability of PEI is improved, which can be either melt-extruded or solution-casted. Although the thermal stability of PEI is lower than PI, i.e., the T_g of PEI is about 217–260 °C, the high temperature capacitive performance of PEI is better than PI. For example, the discharged energy density and the charge/discharge efficiency of PEI are 1.14 J/cm^3 and 82%, respectively, at 150 °C and an applied electric field of 300 MV/m.[49]

FPE synthesized from fluorine bisphenol and phthaloyl chloride [Fig. 1(c)] offers great thermal stability with a T_g of 330 °C and stable dielectric constant up to 300 °C.[50] The discharged energy density and the charge/discharge efficiency of FPE at 150 °C and 300 MV/m are 1.04 J/cm^3 and 58%, respectively,[49] which outperform PI. T_g of FPE can be even increased to 450 °C by chemical modification with a diamond-like hydrocarbon group, i.e., 4,9-diamantyl, which is referred to as FDAPE [Fig. 1(d)].[51] With the introduction of the heterocyclic rings, FDAPE displays a stable dielectric constant of 3.5 and a low dissipation factor of 0.003–0.004 in the temperature range from 25 °C to 350 °C. These features make FDAPE an excellent polymer dielectric for applications in ultra-wide-temperature power electronics.

B. Modification of high temperature dielectric polymers

To improve the dielectric constant and the discharged energy density of PI, various other monomers have been used. One common approach to increase the dielectric constant is to incorporate polar moieties into PI. For example, nitride groups (–CN) have been introduced by the diamine monomer into the backbone of PI.[52–54] It is shown that the presence of –CN group increases the dielectric constant from 2.9 of the nitrile-free PI to 3.1–3.7 of –CN containing PIs, depending on the content of –CN groups.[54] However, the drawback of this strategy is a large variation of the dielectric constant on temperature. Apart from the diamine monomer, changes in the dianhydride monomer can also be used to tune the dielectric constant of PI.[55–58] For instance, different dianhydride monomers of 4,4′-benzophenonetetracarboxylic dianhydride (BTDA), 3,3′,4,4′-biphenyl tetracarboxylic dianhydride (BPDA), 4,4′-oxidiphthalic dianhydride (OPDA), and pyromellitic dianhydride (PMDA), have been used to prepare different PIs [Fig. 2(a)].[58] T_g of the 5,5′-bis(4-aminophenoxy)-2,2′-bipyridine (BPBPA)-based PIs with PMDA, BTDA, BPDA, and OPDA are 320, 296, 285, and 275 °C, respectively, and the corresponding dielectric constants at 220 °C are 5.5, 6.8, 6.4, and 6.0, respectively [Fig. 2(b)].

Simultaneously achieving high dielectric constants and great thermal stability is critical for high temperature polymer dielectrics. However, for most high-temperature dielectric polymers, the relatively low dielectric constant of 2.8–3.5 limits their energy density. To increase the dielectric constant of polymer dielectrics under their T_g, a class of dipolar glass polymers have been developed.[59–62] These dipolar glass polymers utilize the sub-T_g orientation polarization to enhance their dielectric constants. As shown in Fig. 3,

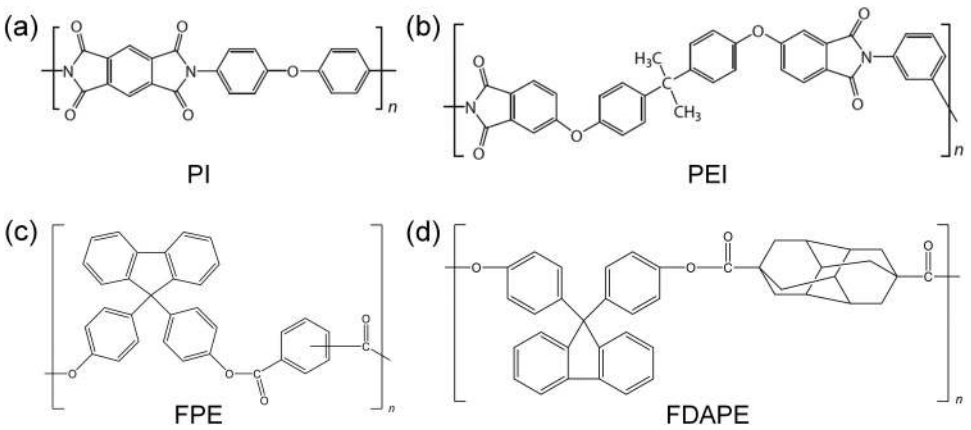

FIG. 1. Chemical structures of (a) polyimide (PI), (b) polyetherimide (PEI), (c) flourene polyester (FPE), and (d) fluorenyl polyester with 4,9-diamantyl group.[51] Reprinted with permission from Venkat *et al.*, Mater. Sci. Eng. B **168**, 16–21 (2010). Copyright 2010 Elsevier.

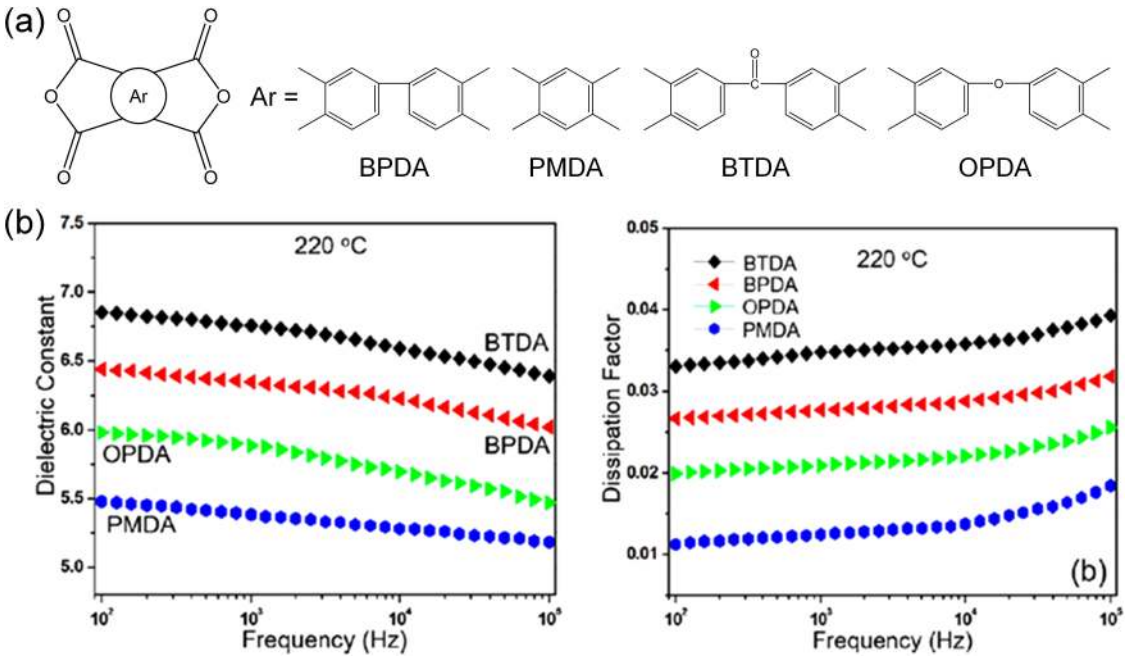

FIG. 2. (a) Chemical structures of various dianhydride monomers for PIs, (b) dielectric constant and dissipation factor of the PIs with various dianhydride at 220 °C.[58] Reprinted with permission from Peng *et al.*, React. Funct. Polym. **106**, 93–98 (2016). Copyright 2016 Elsevier.

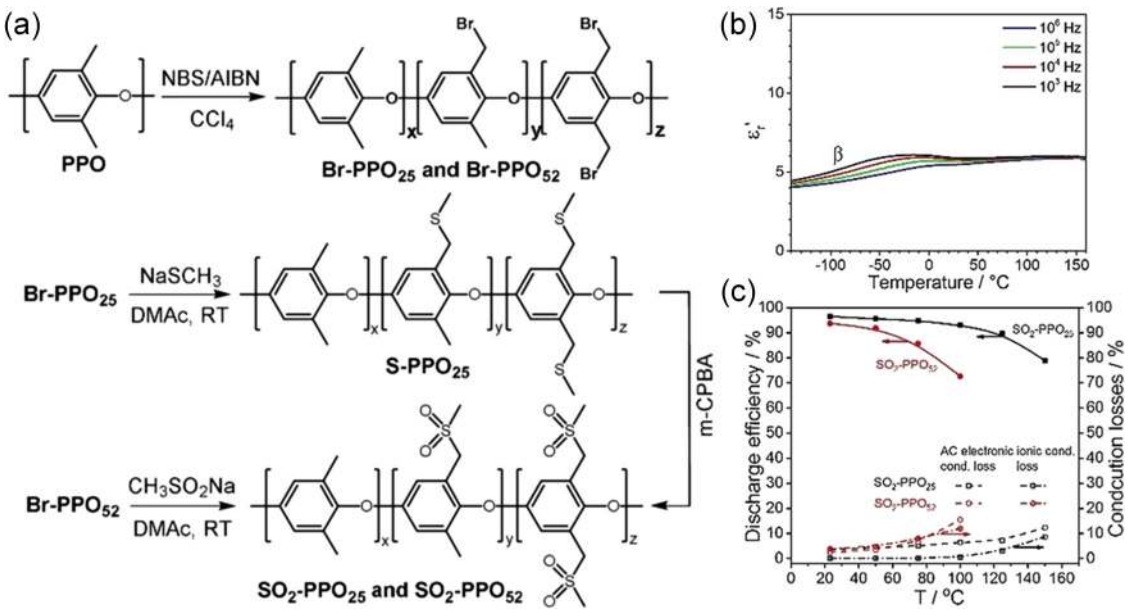

FIG. 3. (a) Synthesis of SO_2-PPOs, (b) temperature dependent dielectric constant of SO_2-PPO, and (c) temperature dependent charge/discharge efficiency of SO_2-PPOs.[62] Reprinted with permission from Zhang *et al.*, Angew. Chem. Int. Ed. **57**, 1528–1531 (2018). Copyright 2018 Wiley-VCH Verlag GmbH & Co. KGaA.

sulfonylated poly(2,6-dimethyl-1,4-phenylene oxide) (SO_2-PPO) is synthesized by post-polymer functionalization.[62] The highly rigid backbone of PPO provides SO_2-PPO with a high T_g of 211 °C. Owing to the effective rotation of highly polar methysulfonyl side groups with the dipole moment of 4.5 D, the dielectric constant of SO_2-PPO reaches 5.9, while the dissipation factor remains as low as 0.003. At 150 °C and an electric field of 300 MV/m, SO_2-PPO can discharge an energy density of 2.2 J/cm^3 with a charge/discharge efficiency of 80%. Further development leads to the sulfonylated polymers with intrinsic microporosity (SO_2-PIM), which pushes the charge/discharge efficiency to 94% under 150 °C and 300 MV/m.[63] The unique combination of relatively high dielectric constant, low dielectric loss, and sufficient thermal stability at a broad temperature window (−50–200 °C) makes this kind of polymer dielectrics promising for high-temperature dielectric applications.

As mentioned in Sec. II, crosslinking is effective not only for improving the thermal stability, but also for suppressing the conduction loss in polymer dielectrics.[64,65] For example, crosslinked fluoropolymer poly(chlorotrifluoroethylene-*co*-vinylidene fluoride) P(CTFE-VDF) is prepared by the melting-processing of the mixture of P(CTFE-VDF), dicumyl peroxide (DCP) as the initiator and triallyl isocyanurate (TAIC) as the co-agent (Fig. 4).[66] The crosslinked P(CTFE-VDF) exhibits much improved discharged energy densities and greater charge/discharge efficiencies, along with excellent breakdown strength and cyclic stability, at elevated temperatures when compared with the current dielectric polymers. For example, the optimized crosslinked P(CTFE-VDF) can deliver an energy density of 2.67 J/cm^3 with a charge/discharge efficiency of >90% at 400 MV/m and 150 °C, which exceeds most high-temperature polymer dielectrics including *c*-BCB, PI, PEI, FPE, SO_2-PPO, and SO_2-PIM and polymer nanocomposites. The comprehensive characterization of conduction current, thermally stimulated current and embedded charges indicates that the crosslinked structure efficiently functions as molecular deep trapping sites to inhabit charge carrier transport and reduce conduction current and thus leads to significantly improved capacitive performance.

Apart from the chemical modification to increase the dielectric constant, physical methods have also been used to improve the dielectric constants via enhancing the dipole–dipole and dipole–environment interactions in the polymers.[67–69] For example, the increased free volume in dipolar polymers at temperatures above T_g can significantly reduce the dipole constraining compared to the glass state. Hence, if the dipole constraining can be deceased at the glassy state, the relatively high dielectric constant may be achieved without compromising the dielectric loss. By combining the effects of the disruption of hydrogen bonds and the improvement of free

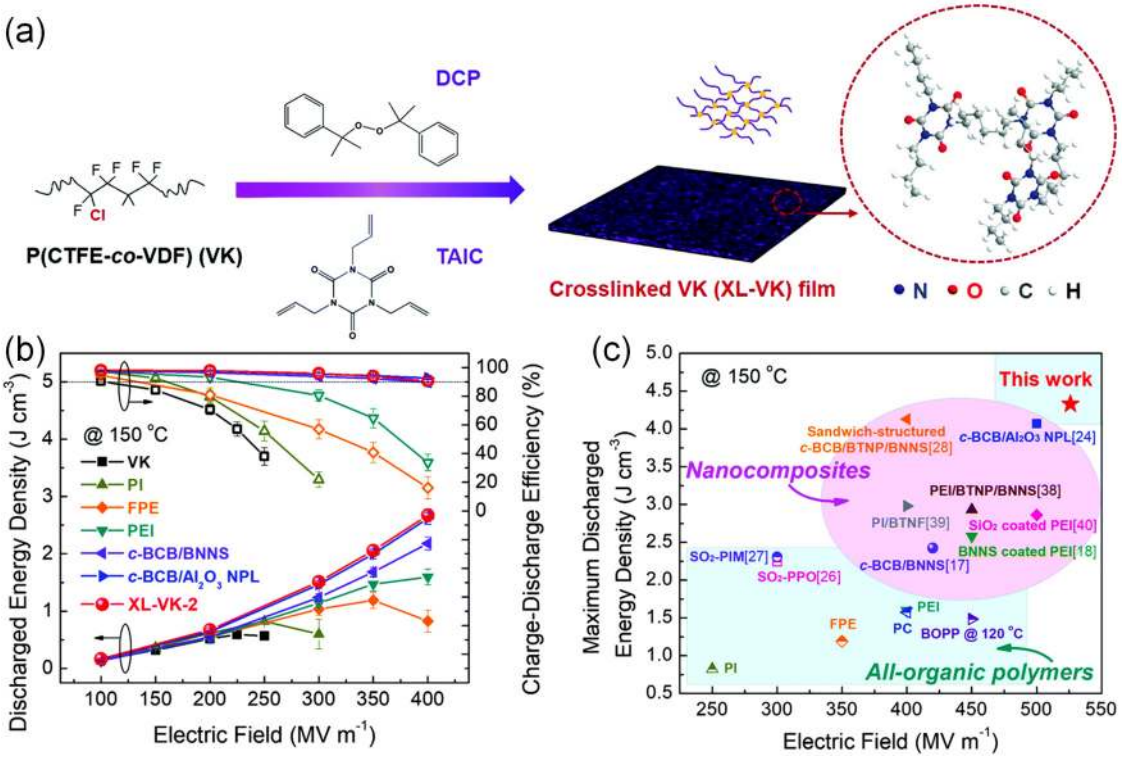

FIG. 4. (a) Schematic of the preparation of crosslinked P(CTFE-VDF)(XL-VK), (b) discharged energy densities and charge/discharge efficiencies of XL-VK and high temperature dielectrics at 150 °C, (c) comparison of the discharged energy density of high-temperature dielectric polymers and polymer composites at 150 °C.[66] Reprinted with permission from Li *et al.*, Energy Environ. Sci. **13**, 1279 (2020). Copyright 2020 The Royal Society of Chemistry.

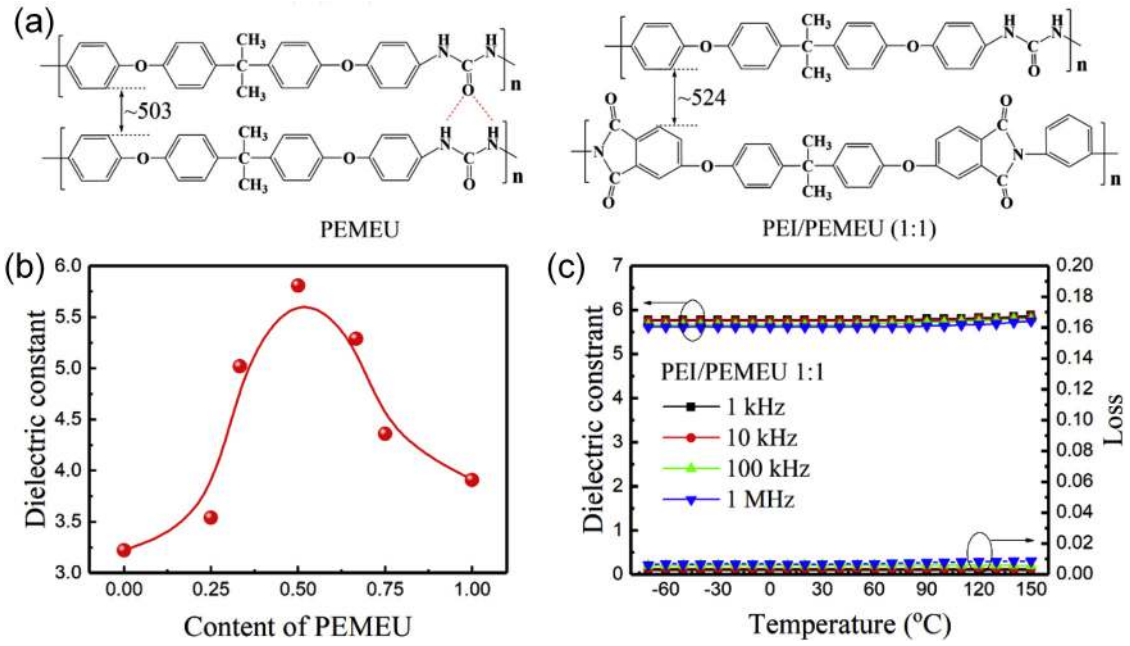

FIG. 5. (a) D-spacing of two parallel molecular chains with different intermolecular interactions in PEMEU and PEI/PEMEU, (b) dielectric constant vs blend composition at room temperature, (c) temperature dependent dielectric properties of 1:1 blend of PEI and PEMEU.[69] Reprinted with permission from Zhang *et al.*, Nano Energy **64**, 103916 (2019). Copyright 2019 Elsevier.

volume,[69] the blend of two high-T_g polymers PEI and poly(ether methyl ether urea) (PEMEU) exhibits a high dielectric constant of 5.8 and a low dissipation factor of <0.01 over a broad temperature range from −70 to 150 °C (Fig. 5).

C. High temperature polymer composites

The polymer nanocomposite approach can integrate the advantages of dielectric polymers, such as high breakdown strength, facile processability, mechanical flexibility, and the unique thermal, mechanical, electrical properties of inorganic fillers to improve the dielectric properties and capacitive performance. For example, the fillers with high dielectric constants, e.g., TiO_2, $BaTiO_3$, $SrTiO_3$, $Ba_xSr_{1-x}TiO_3$, $Pb(Zr_xTi_{1-x})O_3$, and $CaCu_3Ti_4O_{12}$, etc. have been used to increase the dielectric constants of high-temperature polymer dielectrics.[70–77] The introduction of $BaTiO_3$ nanoparticles into PI gives rise to an enhanced dielectric constant of 6.8, and consequently, a discharged energy density of 5.2 J/cm^3 with a charge/discharge efficiency of 86.7% at room temperature.[78] However, the large mismatch of the dielectric constants of $BaTiO_3$ fillers and PI matrix leads to highly distorted local electric fields, and consequently, much reduced breakdown strength. The sharp increase in conduction loss at high temperatures and high electric fields also indicates that comprehensive investigation should be performed to investigate the underlying physical mechanisms of the polymer nanocomposites.

In order to investigate the role of the fillers on the high-temperature capacitive performance of the polymer composites, the PI-based composites containing a series of inorganic fillers (i.e., Al_2O_3, HfO_2, TiO_2 and boron nitride nanosheets) with systematically varied dielectric constants and bandgaps have been prepared (Fig. 6).[79] It is concluded that the bandgap of the fillers dominates the high temperature capacitive performance of the polymer composites at high electric fields. This is in contrast to the polymer composites designed for room-temperature applications at relatively low electric fields, in which the dielectric constant plays a key role. The addition of the fillers with large bandgap significantly reduces the conduction current at high temperatures and high fields, thus yielding high discharged energy densities and great charge/discharge efficiencies. The Al_2O_3 and HfO_2 fillers concomitantly possess large bandgap and moderate dielectric constants exhibit substantial improvement in the breakdown strength, discharged energy density, and charge/discharge efficiency in their respective composites in comparison to the pristine polymer matrix.

Moreover, high-aspect-ratio dopants with highly electrical insulation properties have been adopted to improve the high-temperature capacitive performance of polymer composites.[80–86] The high-aspect-ratio structure of the fillers benefits the polymer composites in the following four aspects. First, a high-aspect-ratio structure is more efficient to reduce the mean free path of the charge carrier and thus suppresses the conduction current. Second, the high-aspect-ratio fillers can provide the resistance to the

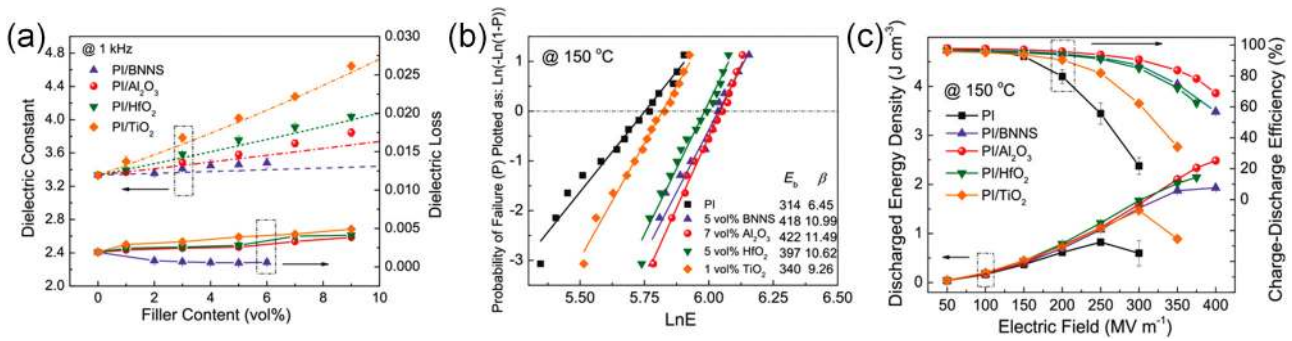

FIG. 6. (a) Dielectric constant and loss of the PI nanocomposites as a function of filler content at 25 °C and 1 kHz, (b) Weibull breakdown strength of PI and the PI nanocomposites with the optimized filler contents measured at 150 °C, (c) discharged energy density and charge/discharge efficiency of PI and the PI nanocomposites at 150 °C.[79] Reprinted with permission from Ai *et al.*, Adv. Energy Mater. **2020**, 1903881 (2020). Copyright 2020 Wiley-VCH Verlag GmbH & Co. KGaA.

electrical tree propagation, which increases the breakdown strength of the polymer composites. Third, the high-aspect-ratio fillers help to mitigate the local electric field concentration at the polymer/filler interfaces. Fourth, the high-aspect-ratio structure reinforces the mechanical properties of the polymer composites and further increases the electrical breakdown strength under high temperatures. For example, boron nitride nanosheets (BNNSs) with a wide bandgap (~6 eV) and high thermal conductivity (~300–2000 W/m K) have been used in the preparation of high-temperature polymer dielectric composites (Fig. 7).[28] The cross-linked divinyltetramethyldisiloxane-bis(benzocyclobutene) *c*-BCB/BNNS composites present substantially reduced high-field electrical conduction at high temperatures, which is more than an order of magnitude less than that of the pristine *c*-BCB. As such, the *c*-BCB/BNNS composites outperform the other high-temperature polymer dielectrics with a record high-temperature capacitive energy storage capability (i.e., breakdown strength of 403 MV/m and a discharged energy density of 1.8 J/cm^3 at 250 °C). Another advantage of BNNSs is the high thermal conductivity, which improves the heat dissipation compared to the pristine polymer. Due to the decreased heat generation arising from lowered conduction current and increased heat dissipation because of improved thermal conductivity, thermal runaway of *c*-BCB/BNNS composite under high temperatures is largely suppressed.

Considering that high-dielectric-constant fillers can improve the dielectric constant and highly insulating fillers can suppress the conduction current, it comes to a strategy of using multi-dopants to simultaneously increase the dielectric constant and breakdown strength.[87–90] The ternary composites consisting of PEI, $BaTiO_3$ nanoparticles and BNNSs have been prepared and optimized by varying the ratio of the dopants (Fig. 8).[91] In the ternary composite with the optimized filler composition, concurrent enhancement in the dielectric constant and breakdown strength has been achieved. The ternary composite achieves an energy density of 2.9 J/cm^3 and breakdown strength of 547 MV/m at 150 °C, which are 83% and 25%, respectively, higher than the pristine polymer.

Recently, a novel design of hierarchically-structured nanofillers has been demonstrated, i.e., chemically or physically tethering the high-dielectric-constant nanoparticles onto the basal plane of insulating nanosheets, e.g., the hierarchically structured nanofillers of $BaTiO_3$@BNNS (Fig. 9).[92,93] With BNNS acting as the insulating barriers to prevent the $BaTiO_3$ nanoparticles from interconnecting, the fluoropolymer/$BaTiO_3$@BNNS composites overcome the adverse impacts of local electric field distortion and high leakage current associated with the incorporation of conventional high-dielectric-constant fillers. The P(VDF-TrFE-CFE)/$BaTiO_3$@BNNS composites exhibit a high discharged energy density of 15.8 J/cm^3 at room temperature, representing a large enhancement of 114% relative to the pristine polymer.[93] Furthermore, the dielectric performance of the polymer composites can be facilely regulated by adjusting the concentration of the nanoparticles and the reaction condition. The two-dimensional (2D) characteristic of the hierarchically structured nanofillers also offers the opportunity to further increase the capacitive performance by aligning the hierarchical nanostructures perpendicularly to the direction of the applied electric field.

Although the composites with BNNSs have shown outstanding high temperature capacitive properties, BNNSs are typically prepared by liquid-phase exfoliation, which is a tedious, low yield, and time consuming process. Therefore, other fillers that can be readily prepared by well-established methods and also have excellent insulating properties have been considered, such as γ-Al_2O_3.[94] Compared to BNNS, γ-Al_2O_3 has a larger bandgap (7.2 eV vs 6.0 eV) and greater dielectric constant (9–10 vs 3–4), along with high breakdown strength of 600–800 MV/m, making it an ideal filler for high-temperature dielectric polymer composites. Among with the γ-Al_2O_3 nanofillers with different morphologies (i.e., nanoparticles, nanowires, and nanoplates), the nanoplates are the most effective in improving the breakdown strength and suppressing the conduction current, which has been confirmed by both experimental and simulation results. The synergistic features of γ-Al_2O_3 nanoplates (Al_2O_3-NPLs) furnish the resultant *c*-BCB/Al_2O_3-NPLs composites with comprehensive advantages, including a very high discharged energy density of 3.3 J/cm^3, a great charge/discharge efficiency of >90%, and remarkable dielectric stability at high electric fields and high temperatures (Fig. 10).

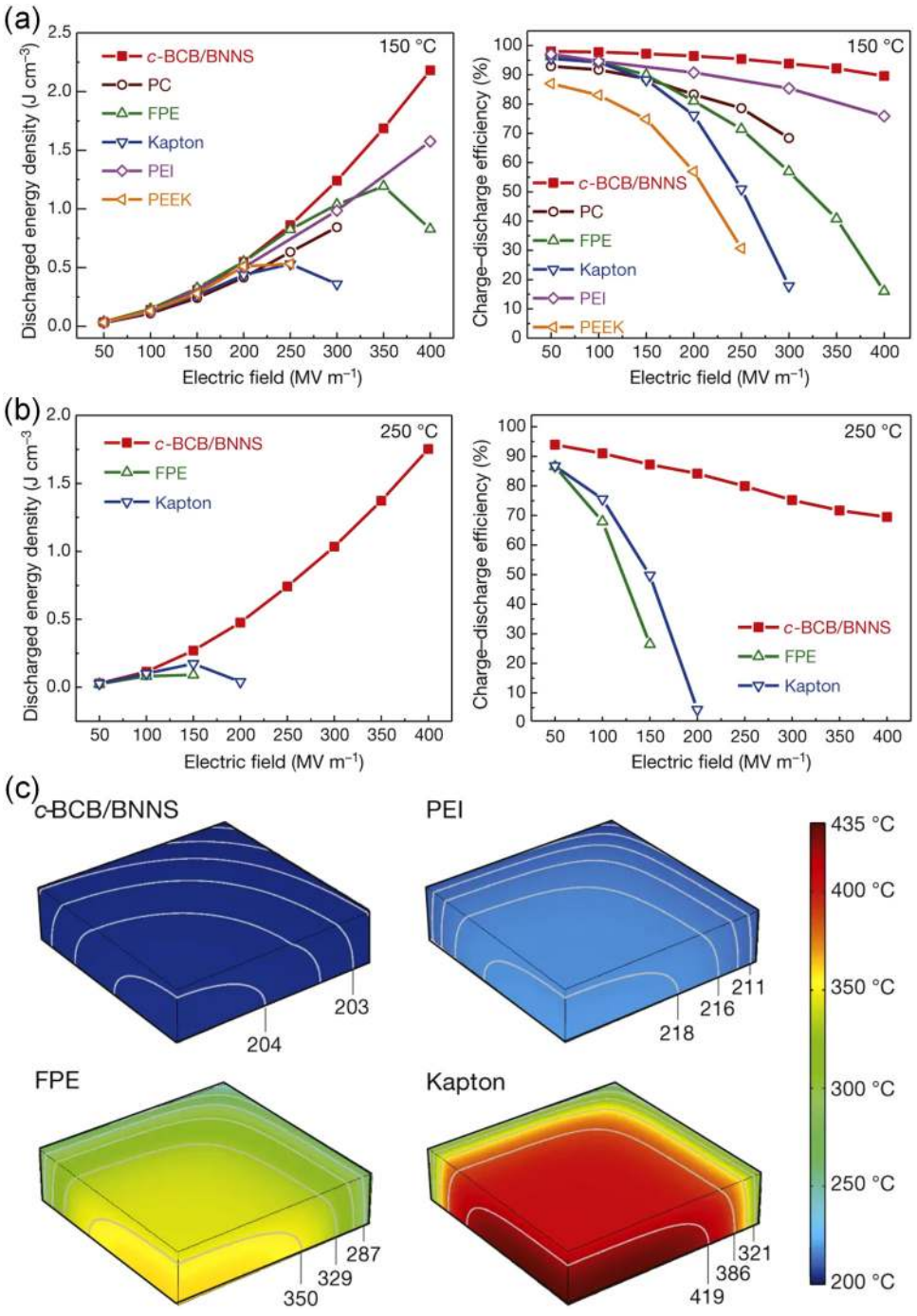

FIG. 7. Discharged energy density and charge/discharge efficiency of *c*-BCB/BNNS composites with 10 vol. % of BNNSs and high-T_g polymer dielectrics measured at (a) 150 °C and (b) 250 °C, (c) simulated steady-state temperature distribution in spiral-wound film capacitors based on *c*-BCB/BNNS with 10 vol. % of BNNSs, PEI, FPE, and PI, respectively.[28] Reprinted with permission from Li *et al.*, Nature **523**, 576–579 (2015). Copyright 2015 Macmillan Publishers Limited.

D. Layer-structured high temperature polymer dielectrics

Although the BNNS-based polymer composites exhibit low dielectric loss, low leakage current, and high breakdown strength at high temperatures, the energy density is still limited by the relatively low dielectric constant. It is thus reasonable to propose a layer-structured polymer composites with several functional layers with complementary properties in order to readily adjust the dielectric properties (i.e., electric polarization, breakdown strength, leakage current, electric field distribution) of the whole film.[95–100]

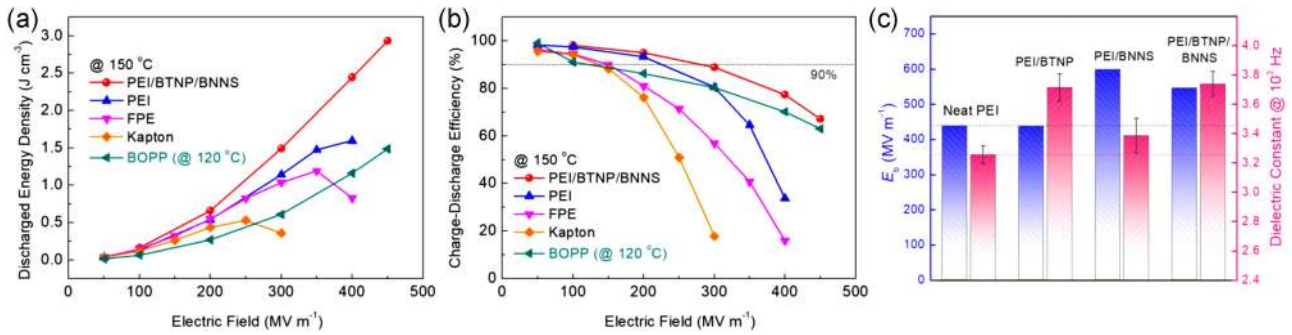

FIG. 8. (a) Discharged energy density and (b) charge/discharge efficiency of ternary PEI nanocomposites and commercial dielectric films at 150 °C, (c) comparison of the Weibull breakdown strength at 150 °C and the dielectric constants of PEI, PEI/$BaTiO_3$, PEI/BNNS, and ternary PEI/ $BaTiO_3$/BNNS nanocomposites at 1 kHz and room temperature.[91] Reprinted with permission from Li *et al.*, InfoMat **2**, 389–400 (2020). Copyright 2020 John Wiley & Sons Australia, Ltd.

For example, the $BaTiO_3$-based composite layer is to increase the dielectric constant, whereas the BNNS-based composite layer is to increase the breakdown strength and inhibit the leakage current. As it is known that BNNS can block the charge injection from the electrodes, which is the main conduction loss mechanism of polymer dielectrics under high electric fields and high temperatures, the optimized architecture has been the arrangement of the high-dielectric-constant layer in the center between two high-insulating BNNS layers. By the introduction of *c*-BCB/$BaTiO_3$ layer in the layered films, the optimized sandwiched (*c*-BCB/BNNS)-(*c*-BCB/$BaTiO_3$)-(*c*-BCB/BNNS) composite film shows an enhanced dielectric constant of 5.8 (Fig. 11).[101] Given that the BNNS-based outer layers can efficiently impede the charge injection from electrodes and introduce deep traps for charge carriers at high temperatures, the trilayered composite film exhibits a discharged energy density of 4 J/cm^3 at 150 °C, which outperforms the *c*-BCB/BNNS composite (~2.2 J/cm^3) measured at the same condition. This investigation provides a novel paradigm of structure design for the layer-structured high-temperature polymer dielectrics.

In addition to the polymer composites layer filled with electrically insulating fillers, coating inorganic layers onto the surface of polymer dielectric films is an emerging approach to the reduction of charge injection and the related energy loss under high temperatures and high electric fields. Chemical vapor deposited *h*-BN with a controlled film thickness has been successfully transferred from copper foil to the surface of PEI film by hot-pressing and substrate etching (Fig. 12).[102] The introduction of the inorganic *h*-BN layers increases the potential barrier due to the small electron affinity of *h*-BN, and thus blocks the charge injection from the electrodes to hinder the conduction current in PEI. The prepared *h*-BN coated PEI films are capable of operating with >90% charge/discharge efficiencies and delivering a high energy density of 1.2 J/cm^3 even at a high temperature (i.e., 200 °C) close to T_g of PEI (i.e., 217 °C). Moreover, the coated *h*-BN shows excellent adhesion and stability with no sign of degradation in the capacitive performance detected over 50 000 charge/discharge cycles, while the pristine PEI film displays noticeable variation in the discharged energy density after 1000th cycles. Other techniques, such as solution casting, magnetron sputtering, and electrospinning,[103–105] have been reported to coat the high-temperature polymer dielectrics with inorganic charge blocking layers.

Alternatively, SiO_2 can be used to coat the surface of polymer dielectric films because of its large bandgap (9 eV) and high breakdown strength (800 MV/m). A roll-to-roll plasma-enhanced chemical vapor deposition (PECVD) approach to coating SiO_2 layers

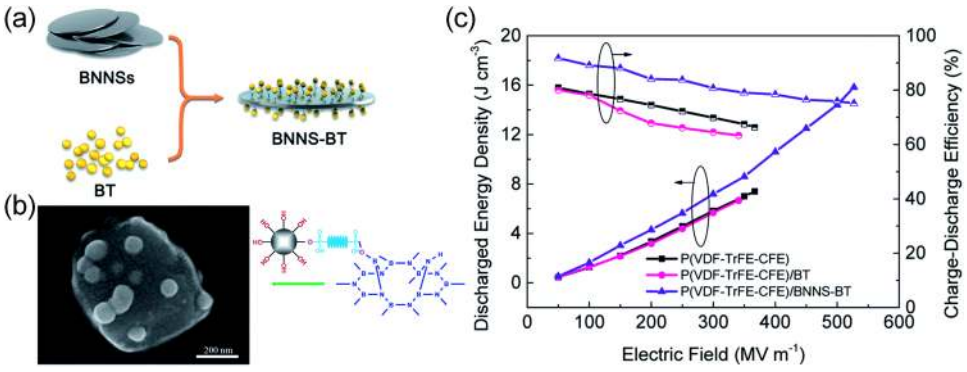

FIG. 9. (a) Schematic of the preparation of $BaTiO_3$@BNNS hierarchically-structured nanofillers, (b) SEM image of $BaTiO_3$@BNNS nanofillers, (c) discharged energy density and charge/discharge efficiency of P(VDF-TrFE-CFE), P(VDF-TrFE-CFE)/$BaTiO_3$ and P(VDF-TrFE-CFE)/$BaTiO_3$@BNNS at room temperature.[93] Reprinted with permission from Li *et al.*, J. Mater. Chem. A **8**, 6576 (2020). Copyright 2020 The Royal Society of Chemistry.

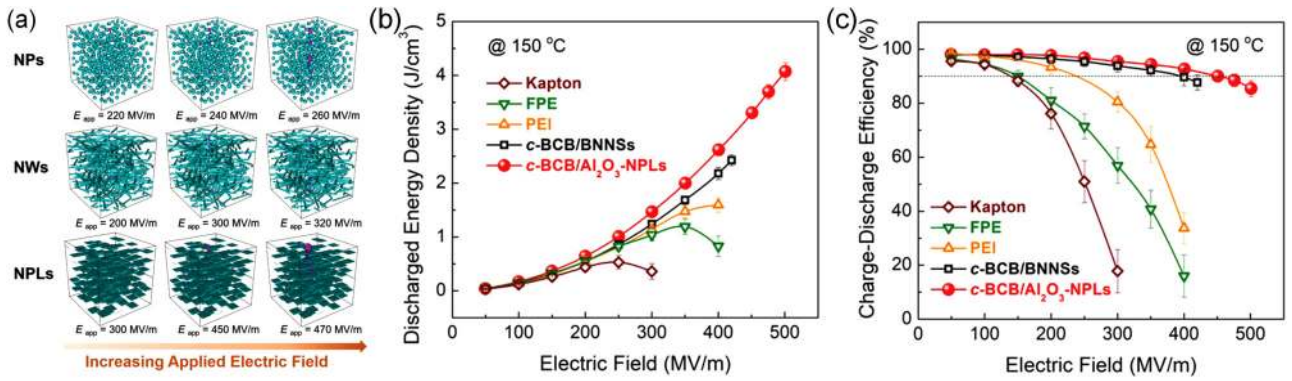

FIG. 10. (a) The predicted breakdown path evolution computed by phase-field simulations of the *c*-BCB nanocomposites with 7.5 vol. % Al_2O_3 nanoparticles, nanowires and nanosheets at 150 °C and varied applied electric fields, (b) discharged energy density and (c) charge/discharge efficiency of high-temperature dielectric polymers and the *c*-BCB nanocomposites measured at 150 °C.[94] Reprinted with permission from Li *et al.*, Adv. Mater. **31**, 1900875 (2019). Copyright 2019 Wiley-VCH Verlag GmbH & Co. KGaA.

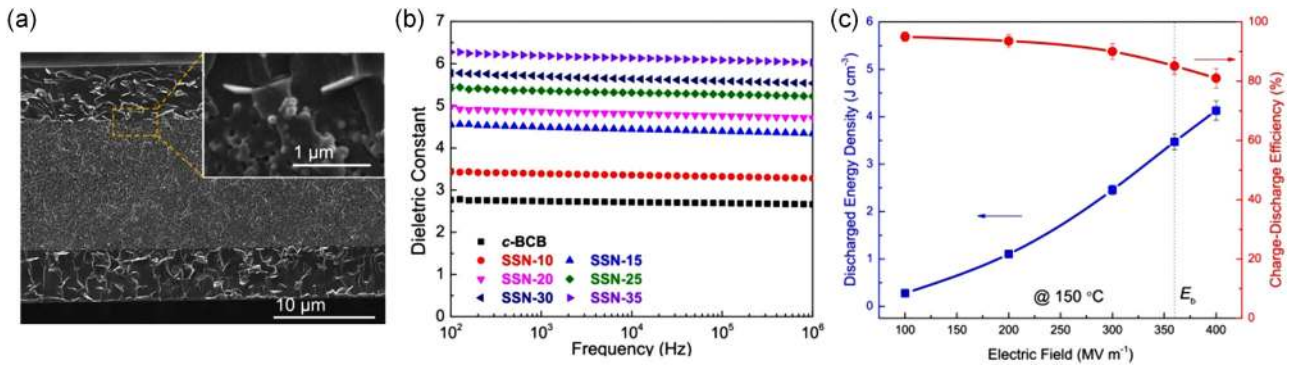

FIG. 11. (a) Cross-sectional SEM image of sandwich-structured nanocomposites, (b) frequency-dependent dielectric constant of the sandwich-structured nanocomposites with varied $BaTiO_3$ contents in the middle layer measured at room temperature, (c) discharged energy density and charge/discharge efficiency of the sandwich-structured nanocomposites measured at 150 °C.[101] Reprinted with permission from Li *et al.*, Proc. Natl. Acad. Sci. U.S.A. **113**, 9995–10000 (2016). Copyright 2016 National Academy of Sciences.

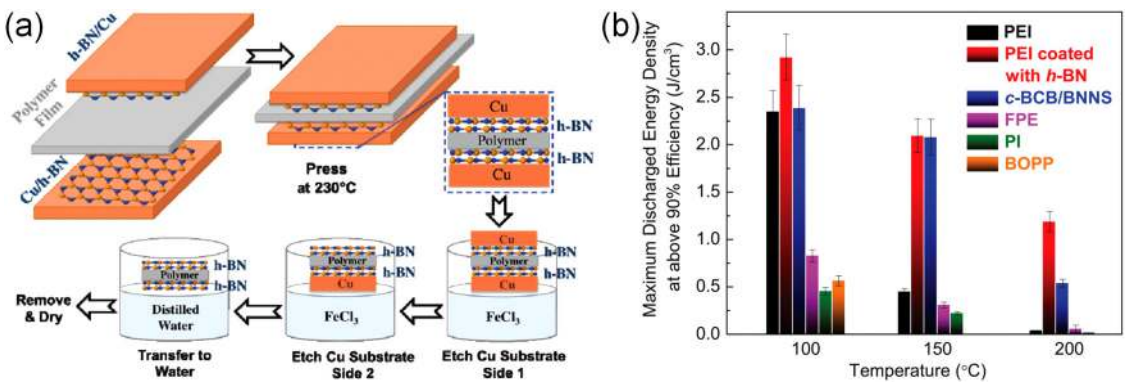

FIG. 12. (a) Schematics of the transfer process of the CVD-grown h-BN films onto the polymer films, (b) discharged energy density achieved at above 90% charge/discharge efficiencies at varied temperatures.[102] Reprinted with permission from Azizi *et al.*, Adv. Mater. **29**, 201701864 (2017). Copyright 2017 Wiley-VCH Verlag GmbH & Co. KGaA.

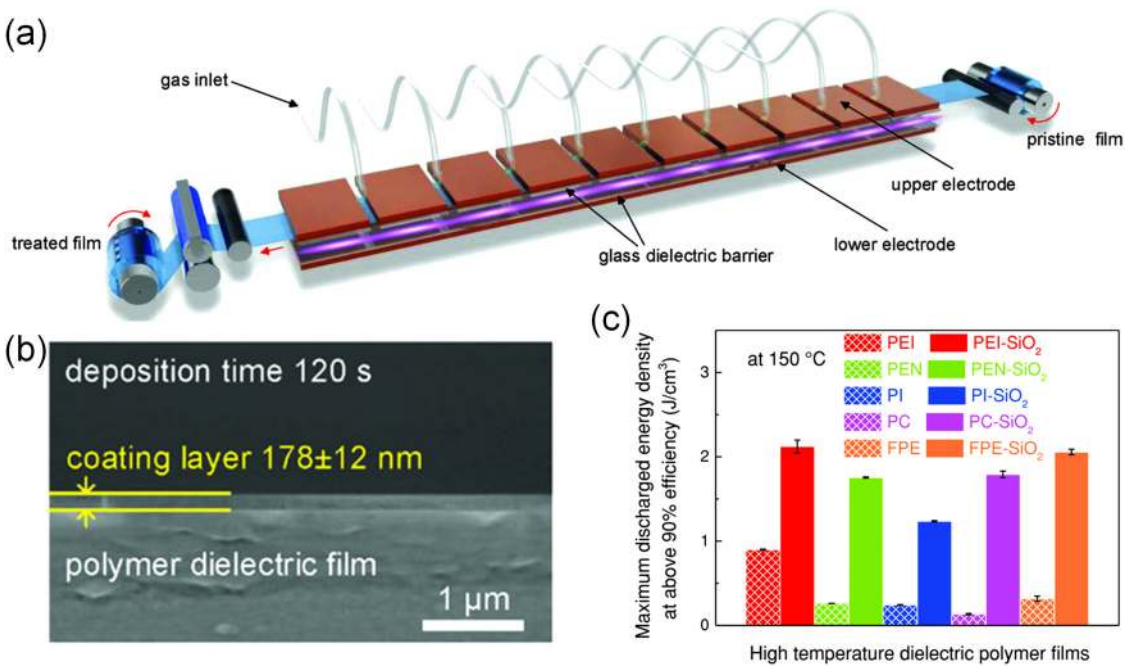

FIG. 13. (a) Schematic of the roll-to-roll PECVD, (b) cross-sectional SEM image of the coating layer on polymer film, (c) the maximum discharged energy density of the various dielectric films before and after coating achieved at above 90% charge/discharge efficiencies measured at 150 °C.[49] Reprinted with permission from Zhou *et al.*, Adv. Mater. **30**, 201805672 (2018). Copyright 2018 Wiley-VCH Verlag GmbH & Co. KGaA.

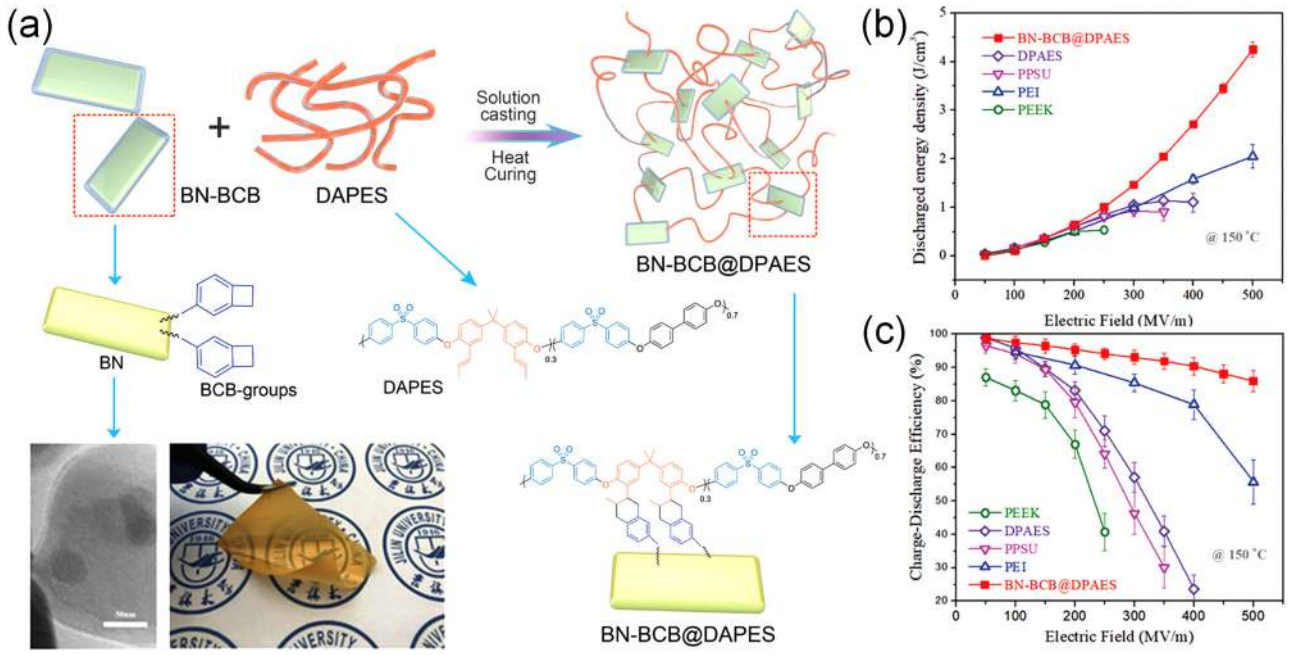

FIG. 14. (a) Schematic of the preparation of BN-BCB@DPAES films, (b) discharged energy density and (c) charge/discharge efficiency of the dielectrics as a function of the applied electric fields at 150 °C.[29] Reprinted with permission from Xu *et al.*, Small **28**, 201901582 (2019). Copyright 2019 Wiley-VCH Verlag GmbH & Co. KGaA.

onto various high temperature polymer dielectric films (i.e., PEI, PEN, PI, PC, and FPE) has been proposed (Fig. 13).[49] The uniformly deposited SiO_2 layer increases the potential barrier at the electrode/dielectric interface, and consequently impedes the charge injection and yields highly decreased conduction current, which enables the substantially improved high-temperature capacitive performance of the coated films in comparison to the pristine polymer films. It is more noteworthy that the roll-to-roll processing under ambient condition without generating any toxic chemicals as side products allows the scalable, high-throughput, and environmentally benign modification of various polymer dielectric films. This approach offers a pathway to the general and scalable production of surface-functionalized high-temperature polymer dielectric films, which has been one of the key challenges in this field.

E. Interface modulation in high temperature polymer composites

It has been demonstrated that both the physical and chemical properties of the nanoparticles and their interaction with polymer matrix are critical to the microstructures and overall properties of the polymer composites. To address the mismatch of the physical and chemical properties between the inorganic nanoparticles and organic polymer matrix, various surface modification approaches of the inorganic fillers have been proposed to improve the

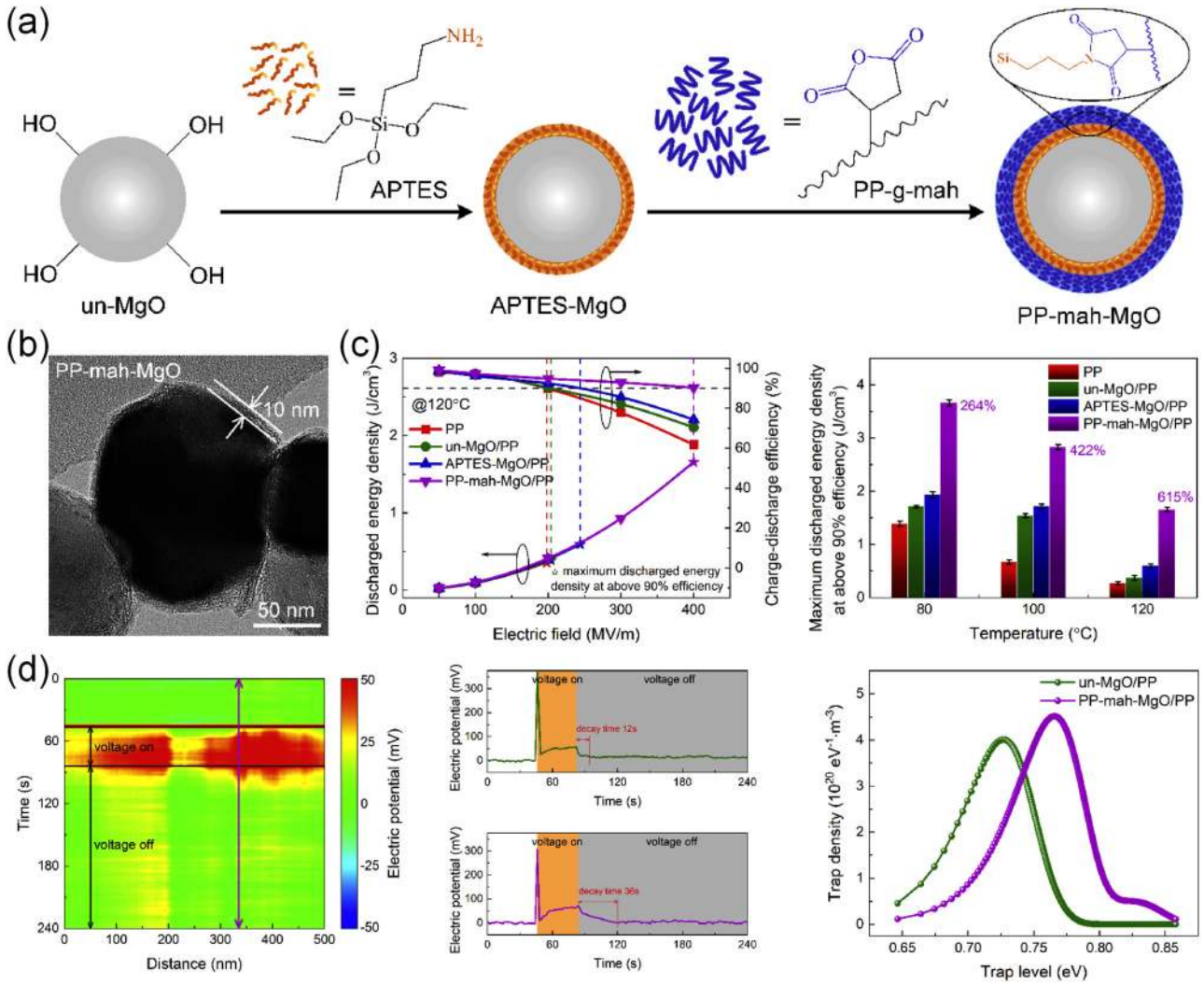

FIG. 15. (a) Schematic of the preparation of PP-mah-MgO nanoparticles, (b) TEM images of PP-mah-MgO nanoparticles, (c) high-temperature energy storage performance of PP and the PP nanocomposites, (d) local charge trap level distribution characterized by Kelvin probe force microscopy.[110] Reprinted with permission from Zhou *et al.*, Energy Stor. Mater. **28**, 255–263 (2020). Copyright 2020 Elsevier.

interfacial compatibility between the polymers and nanofillers to achieve desired performance.[106–109]

Inspired by the hierarchical nanostructure of spider silk, BNNSs are first surface modified with reactive functional groups of BCB by heck coupling reaction and then followed by the Diels–Alder reaction of the BCB group on BNNS and the propenyl groups in a poly(aryl ether sulfone) (DAPES) matrix (Fig. 14).[29] Owing to the excellent thermal stability of both DAPES polymer and BCB modified BNNS fillers, as well as the nanoconfinement effect of the hierarchical interfacial structure, the mechanical and electrical properties of the resultant polymer composites have been greatly improved. The discharged energy density of 2.7 J/cm^3 and a charge/discharge efficiency of >90% are simultaneously achieved at 150 °C and 400 MV/m.

Although heat-resistant polymers and their composites have been reported to show decent high temperature capacitive performance, these materials are much more expensive than the capacitive grade polypropylene (PP) film which is the best commercially available dielectric polymer. Moreover, there is a distinct lack of production maturity of the heat-resistant polymers to achieve the productivity and film quality when compared to that of the PP-based capacitor films. However, the commercial BOPP film can only operate below 105 °C, which is much lower than the requirements of many harsh environment applications. In order to improve the high temperature (e.g., 120 °C) capacitive performance of the PP-based materials, interface modulation of the PP-based nanocomposites is proposed (Fig. 15).[110] The embedded MgO nanoparticles are functionalized with a layer of polypropylene-graft-maleic anhydride (PP-*g*-mah) that is miscible with the PP matrix to substantially increase the compatibility and avoid the structural defects at the interface. The polar coating layer with a dielectric constant of ~6 of PP-*g*-mah not only benefits the improvement in the dielectric constant of the polymer composites but also offers deep traps to suppress the electrical conduction. The resultant PP-based polymer composites display a discharged energy density of 1.66 J/cm^3 (i.e., 615% that of the pristine PP film) and a charge-discharge efficiency of >90% at 400 MV/m and 120 °C. It should be noted that the local deep charge traps introduced by the modulated interfaces are directly detected and quantitatively probed by the *in situ* characterization using Kelvin probe force microscopy. The microscopic material characterization provides a powerful tool to directly measure the properties of the interfaces in polymer nanocomposites, which has been hardly accessible by using conventional bulk material characterization techniques.

More recently, it is revealed that a very low volume content of nanofillers in high-temperature semicrystalline dipolar polymer, poly(arylene ether urea) (PEEU), can generate more than 50% increase in the dielectric constant.[111] For instance, the addition of only 0.2 vol. % of Al_2O_3 nanoparticles increases the dielectric constant from 4.7 of the PEEU polymer to 7.4 of the PEEU/Al_2O_3

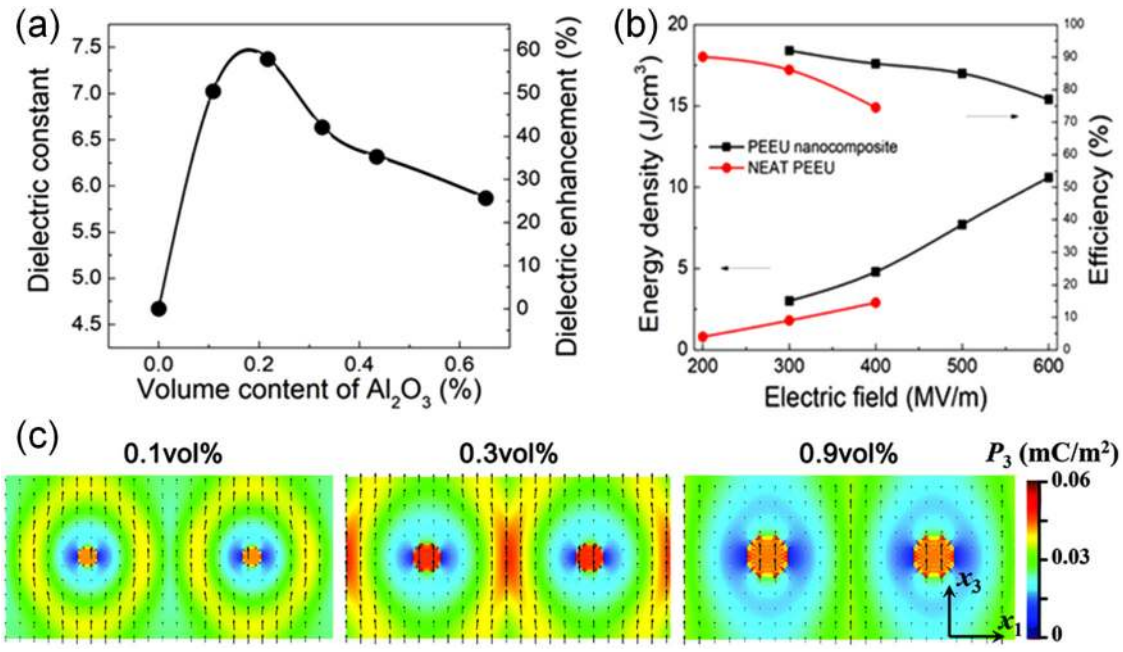

FIG. 16. (a) Dielectric constant at 1 kHz vs the Al_2O_3 nanofiller loading content in PEEU/Al_2O_3 nanocomposites, (b) discharged energy density and charge/discharge efficiency as a function of applied electric fields for the base PEEU and nanocomposite with 0.21 vol. % alumina at 150 °C.[112] Reprinted with permission from Zhang *et al.*, Sci. Adv. **6**, eaax6622 (2020). Copyright 2020 American Association for the Advancement of Science. (c) Polarization distribution in PEI/Al_2O_3 nanocomposites with nanofillers of 20 nm at filler contents of 0.1 vol. %, 0.3 vol. %, and 0.9 vol. %.[111] Reprinted with permission from Thakur *et al.*, Nanoscale **9**, 10992 (2017). Copyright 2017 The Royal Society of Chemistry.

composites (Fig. 16).[112] These results are different from the conventional wisdom that large contents of high dielectric constant fillers are preferred in order to improve the dielectric constant of polymer composites. The improved dielectric constant of the PEEU/Al_2O_3 composite is attributed to the generation of local and nanostructure changes that weaken the hydrogen bonding and expand the interchain spacing, which create local free volume and reduce local dipole constrains of the PEEU polymer matrix. Moreover, the low loading nanofillers also substantially reduce the high-field conduction loss because of the enhanced deep trap level, increased crystallinity, and reduced crystalline size. Consequently, the prepared polymer composite displays a high discharged energy density of 5 J/cm^3 with a high charge/discharge efficiency at 150 °C. Although the improved capacitive performance, especially the increased dielectric constant, has been explained by macroscopic characterization and computational simulation, direct microscopic evidence and mechanisms are still lacking, which warrants further research.

IV. CONCLUSION AND FUTURE PERSPECTIVES

There have been exciting developments in the field of high-temperature polymer dielectrics in recent years. Various types of high-temperature polymer dielectrics including polymers and polymer composites, as well as prototypes of advanced film processing technologies have been developed, which provide a solid foundation for the industrial development and applications of high-performance high-temperature polymer dielectric films. Particularly, some of the developed films have shown unprecedented high-temperature capacitive energy storage performance, which can potentially meet the requirements of practical harsh-environment applications. Although great achievements have been made, there is still plenty of room for further improvement and significant challenges remain from both fundamental and practical points of view. Further developments of high-temperature polymer dielectrics should mainly consider, but are not limited to, the following aspects: (a) improvement of the fundamental understanding of the structure–property relationship, (b) rational design of the material and film structures based on the underlying physical mechanisms, particularly the high-temperature high-field electrical conduction and dielectric behavior of polymeric materials, and (c) scalable production of the developed high-performance high-temperature polymer dielectrics with capacitive film quality.

Future structural optimization of high-temperature polymer dielectrics should balance the thermal stability, dielectric properties, mechanical flexibility, and film processability. In-depth fundamental research should be carried out on the relationship between the chemical structures and physical properties in polymer dielectrics, which can provide guidance on the rational structure design. Note that the majority of the high-performance high-temperature polymer dielectrics are currently based on the composite approach. There is an urgent need to develop all-polymer based high-temperature dielectrics because of their intrinsic processing advantages and maturity in the industrial scales. Computational simulation as well as machine learning and big data technology can further assist the design of new polymer structures.

The current high temperature polymer dielectrics usually possess relatively low dielectric constant, i.e., below 4, which severely restricts their stored energy densities. Traditional design criteria of dielectric polymer composites for ambient-temperature applications via introducing high-dielectric-constant fillers are not applicable for high-temperature applications because the conduction loss increases nonlinearly under high temperatures and high electric fields. To address this issue, there are two potential approaches, one is to modify the molecular structure of polymers, such as introducing polar groups, the other is the topological structure optimization, such as layer-structured polymers and polymer composites. Different from the traditional polymer composites with the homogeneous composition and nanoparticle distribution, the topologically structured optimization allows the polymers and polymer composites to have layered structures or graded nanoparticle distribution. Such a topological structure enables the different layers to have different functionalities, e.g., high dielectric constant layer, high breakdown strength layer, and high electron resistance layer. By optimization of the layer assembly and nanoparticle distribution, the performance of the high temperature polymer dielectrics can be further improved.

Polymer nanocomposites which integrate the advantages of both organic and inorganic components are promising to achieve high-performance high-temperature polymer dielectrics. Further decreasing the loading fraction of fillers to maintain good mechanical flexibility and processability is a key issue to be solved. For dielectric nanocomposites, low-cost scalable production remains a great challenge. Moreover, the microscopic mechanisms and the interfacial coupling effect in dielectric polymer nanocomposites are important fundamental research topics that need to be investigated. For example, it remains unclear how the inorganic and organic dipoles interact at the interface and contribute to the overall polarization of the composites, as well as the role of the so-called interfacial coupling effect in high-field high-temperature dielectric properties of the composites. Novel electronic microscopic techniques need to be developed to image and quantify the polarization and electric field distribution in the polymer composites, especially at the organic/inorganic interface.

As a highly interdisciplinary field, the progress in high-temperature dielectric polymers is critically dependent on our fundamental understanding of the electrical and dielectric properties of polymers at elevated temperatures and high electric fields. The successful interactions across the boundaries of traditional disciplines including chemistry, materials science and engineering, applied physics, electrical engineering, and computational and data science would not only promote the development of high-performance polymer dielectrics but also open up more interesting opportunities in applied physics and technological applications in the near future.

ACKNOWLEDGMENTS

This work was supported by the U.S. Office of Naval Research (ONR) under Grant No. N00014-11-1-0342.

DATA AVAILABILITY

The data that support the findings of this study are available from the corresponding author upon reasonable request.

REFERENCES

[1]W. J. Sarjeant, J. Zirnheld, and F. W. MacDougall, IEEE Trans. Plasma Sci. **26**, 1368 (1998).
[2]W. J. Sarjeant, I. W. Clelland, and R. A. Price, Proc. IEEE **89**, 846 (2001).
[3]Q. Tan, P. Irwin, and Y. Cao, IEEJ. Trans. Fundam. Mater. **26**, 1152 (2006).
[4]A. J. Bell, J. Eur. Ceram. Soc. **28**, 1307 (2008).
[5]D. Montanari, K. Saarinen, F. Scagliarini, D. Zeidler, M. Niskala, and D. Nender, "Film capacitors for automotive and industrial applications," in Proceedings of CARTS USA 2009 (Electronic Components Industry Association, 2009), pp. 23–38.
[6]W. Bower, Prog. Photovoltaics **8**, 113 (2000).
[7]R. W. Johnson, J. L. Evans, P. Jacobsen, J. R. R. Thompson, and M. Christopher, IEEE Trans. Electron. Packag. Manuf. **27**, 164 (2004).
[8]B. Chu, X. Zhou, K. Ren, B. Neese, M. Lin, Q. Wang, F. Bauer, and Q. M. Zhang, Science **313**, 334 (2006).
[9]P. Khanchaitit, K. Han, M. R. Gadinski, Q. Li, and Q. Wang, Nat. Commun. **4**, 2845 (2013).
[10]L. Zhu, J. Phys. Chem. Lett. **5**, 3677 (2014).
[11]M. S. Islam, Y. Qiao, C. Tang, and H. J. Ploehn, ACS Appl. Mater. Interfaces **7**, 1967 (2015).
[12]J. Pan, K. Li, J. Li, T. Hsu, and Q. Wang, Appl. Phys. Lett. **95**, 022902 (2009).
[13]D. Tan, L. Zhang, Q. Chen, and P. Irwin, J. Electron. Mater. **43**, 4569 (2014).
[14]J. A. Weimer. "Electrical power technology for the more electric aircraft," in 12th Proceedings of AIAA/IEEE Digital Avionics Systems Conference (IEEE, 1993), pp. 445–450.
[15]J. Watson and G. Castro, Analog Dialogue **46**, 1 (2012).
[16]E. J. Barshaw, J. White, M. J. Chait, J. B. Cornette, J. Bustamante, F. Folli, D. Biltchick, G. Borelli, G. Picci, and M. Rabuffi, IEEE Trans. Magn. **43**, 223 (2007).
[17]M. Rabuffi and G. Picci, IEEE. Trans. Plasma Sci. **30**, 1939 (2002).
[18]S. Zhang, C. Zou, D. I. Kushner, X. Zhou, R. J. Orchard, N. Zhang, and Q. M. Zhang, IEEE Trans. Dielectr. Electr. Insul. **19**, 1158 (2012).
[19]T. A. Burress, C. L. Coomer, S. L. Campbell, A. A. Wereszczak, J. P. Cunningham, L. D. Marlino, L. E. Seiber, and H. T. Lin, "Evaluation of the 2008 Lexus LS 600H hybrid synergy drive system," Technical Report ORNL/TM-2008/185, Oak Ridge National Laboratory, 2009.
[20]T. A. Burress, C. L. Coomer, S. L. Campbell, L. E. Seiber, L. D. Marlino, R. H. Staunton, and J. P. Cunningham, Evaluation of the 2007 Toyota Camry hybrid synergy drive system," Technical Report ORNL/TM-2007/190, Oak Ridge National Laboratory, 2007.
[21]J. S. Hsu, M. R. Staunton, and M. R. Starke, "Barriers to the application of high-temperature coolants in hybrid electric vehicles," Technical Report ORNL/TM-2006/514, Oak Ridge National Laboratory, 2006.
[22]Q. Li, F. Z. Yao, Y. Liu, G. Zhang, H. Wang, and Q. Wang, Annu. Rev. Mater. Res. **48**, 219 (2018).
[23]D. Q. Tan, Adv. Funct. Mater. **30**, 1808567 (2020).
[24]B. Fan, F. Liu, G. Yang, H. Li, G. Zhang, S. Jiang, and Q. Wang, IET Nanodielectrics **1**, 32 (2018).
[25]J. S. Ho and S. G. Greenbaum, ACS Appl. Mater. Interfaces **10**, 29189 (2018).
[26]J. Pan, K. Li, S. Chuayprakong, T. Hsu, and Q. Wang, ACS Appl. Mater. Interfaces **2**, 1286 (2010).
[27]R. Yang, R. Wei, K. Li, L. Tong, K. Jia, and X. Liu, Sci. Rep. **6**, 36434 (2016).
[28]Q. Li, L. Chen, M. R. Gadinski, S. Zhang, G. Zhang, H. U. Li, E. Iagodkine, A. Haque, L. Q. Chen, T. N. Jackson, and Q. Wang, Nature **523**, 576 (2015).
[29]W. Xu, J. Liu, T. Chen, X. Jiang, X. Qian, Y. Zhang, Z. Jiang, and Y. Zhang, Small **15**, 1901582 (2019).
[30]Q. Chen, Y. Shen, S. Zhang, and Q. M. Zhang, Annu. Rev. Mater. Res. **45**, 433 (2015).
[31]T. D. Huan, S. Boggs, G. Teyssedre, C. Laurent, M. Cakmak, S. Kumar, and R. Ramprasad, Prog. Mater. Sci. **83**, 236 (2016).
[32]M. Ieda, IEEE Trans. Dielectr. Electr. Insul. **E1–E15**, 206 (1980).
[33]K. H. Stark and C. G. Garton, Nature **176**, 1225 (1955).
[34]N. Zebouchi, M. Bendaoud, R. Essolbi, D. Malec, B. Ai, and H. Giam, J. Appl. Phys. **79**, 2497 (1996).
[35]T. L. Hanley, B. P. Burford, R. J. Fleming, and K. W. Barber, IEEE Electr. Insul. Mag. **19**, 13 (2003).
[36]M. Ieda, IEEE Trans. Electr. Insul. **EI-19**, 162 (1984).
[37]M. Huang, Y. Zhou, Z. Zhou, and B. Qi, Energies **10**, 2160 (2017).
[38]F. C. Chiu, Adv. Mater. Sci. Eng. **2014**, 578168 (2014).
[39]J. Ho and T. R. Jow, IEEE Trans. Dielectr. Electr. Insul. **19**, 990 (2012).
[40]M. Ieda, IEEE Trans. Electr. Insul. **E1–E19**, 162 (1984).
[41]V. Ambegaokar, B. I. Halperin, and J. S. Langer, Phys. Rev. B **4**, 2612 (1971).
[42]R. J. Young and P. A. Lovell, *Introduction to Polymers* (Chapman & Hall, London, 1991).
[43]X. Huang, P. Jiang, and T. Tanaka, IEEE Electr. Insul. Mag. **27**, 8 (2011).
[44]M. Xiao and B. X. Du, High Voltage **1**, 34 (2016).
[45]Z. Han and A. Fina, Prog. Polym. Sci. **36**, 914 (2011).
[46]I. A. Tsekmes, R. Kochetov, P. H. F. Morshuis, and J. J. Smit, "Thermal conductivity of polymeric composites: A review," in 2013 IEEE International Conference on Solid Dielectrics (IEEE, 2013), pp. 678–681.
[47]A. J. Kirby, *Polyimides: Materials Processing and Applications* (Pergamon Press, Oxford, 1992).
[48]K. Vanherck, G. Koeckelberghs, and I. F. J. Vankelecom, Prog. Polym. Sci. **38**, 874 (2013).
[49]Y. Zhou, Q. Li, B. Dang, Y. Yang, T. Shao, H. Li, J. Hu, R. Zeng, J. He, and Q. Wang, Adv. Mater. **30**, 1805672 (2018).
[50]J. Edward Hampl, "3M high temperature dielectric film," in 2nd NASA Workshop on Wiring for Space Applications (NASA, 1993), pp. 203–210.
[51]N. Venkat, T. D. Dang, Z. Bai, V. K. McNier, J. N. DeCerbo, B. H. Tsao, and J. T. Stricker, Mater. Sci. Eng. B **168**, 16 (2010).
[52]D. H. Wang, J. K. Riley, S. P. Fillery, M. F. Durstock, R. A. Vaia, and L. S. Tan, J. Polym. Sci. Part A Polym. Chem. **51**, 4998 (2013).
[53]D. H. Wang, B. A. Kurish, I. Treufeld, L. Zhu, and L. S. Tan, J. Polym. Sci. Part A Polym. Chem. **53**, 422 (2015).
[54]I. Treufeld, D. H. Wang, B. A. Kurish, L. S. Tan, and L. Zhu, J. Mater. Chem. A **2**, 20683 (2014).
[55]R. Ma, A. F. Baldwin, C. Wang, I. Offenbach, M. Cakmak, R. Ramprasad, and G. A. Sotzing, ACS Appl. Mater. Interfaces **6**, 10445 (2014).
[56]A. F. Baldwin, R. Ma, C. Wang, R. Ramprasad, and G. A. Sotzing, J. Appl. Polym. Sci. **130**, 1276 (2013).
[57]X. Peng, Q. Wu, S. Jiang, M. Hanif, S. Chen, and H. Hou, J. Appl. Polym. Sci. **131**, 40828 (2014).
[58]X. Peng, W. Xu, L. Chen, Y. Ding, T. Xiong, S. Chen, and H. Hou, React. Funct. Polym. **106**, 93 (2016).
[59]J. Wei, Z. Zhang, J. K. Tseng, I. Treufeld, X. Liu, M. H. Litt, and L. Zhu, ACS Appl. Mater. Interfaces **7**, 5248 (2015).
[60]J. F. Legrand, B. Daudin, and E. Bellet-Amalric, Nucl. Instrum. Meth. B **105**, 225 (1995).
[61]Y. F. Zhu, Z. Zhang, M. H. Litt, and L. Zhu, Macromolecules **51**, 6257 (2018).
[62]Z. Zhang, D. H. Wang, M. H. Litt, L. S. Tan, and L. Zhu, Angew. Chem. Int. Ed. **130**, 1544 (2018).
[63]Z. Zhang, J. Zheng, K. Premasiri, M. H. Kwok, Q. Li, R. Li, S. Zhang, M. H. Litt, X. P. A. Gao, and L. Zhu, Mater. Horiz. **7**, 592 (2020).
[64]S. Chen, G. Meng, B. Kong, B. Xiao, Z. Wang, Z. Jing, Y. Gao, G. Wu, H. Wang, and Y. Cheng, Chem. Eng. J. **387**, 123662 (2020).
[65]X. Yuan and T. M. Chung, Appl. Phys. Lett. **98**, 062901 (2011).
[66]H. Li, M. R. Gadinski, Y. Huang, L. Ren, Y. Zhou, D. Ai, Z. Han, B. Yao, and Q. Wang, Energy Environ. Sci. **13**, 1279 (2020).
[67]Y. Thakur, B. Zhang, R. Dong, W. Lu, C. Iacob, J. Runt, and J. Bernholc, Nano Energy **32**, 73 (2017).
[68]Y. Thakur, R. Dong, M. Lin, S. Wu, Z. Cheng, Y. Hou, J. Bernholc, and Q. M. Zhang, Nano Energy **16**, 227 (2015).
[69]Q. Zhang, X. Chen, T. Zhang, and Q. M. Zhang, Nano Energy **64**, 103916 (2019).

[70]J. Li, S. I. Seok, B. Chu, F. Dogan, Q. Zhang, and Q. Wang, Adv. Mater. **21**, 217 (2009).
[71]W. Xu, G. Yang, L. Jin, J. Liu, Y. Zhang, Z. Zhang, and Z. Jiang, ACS Appl. Mater. Interfaces **10**, 11233 (2018).
[72]Z. M. Dang, Y. Q. Lin, H. P. Xu, C. Y. Shi, S. T. Li, and J. Bai, Adv. Funct. Mater. **18**, 1509 (2008).
[73]L. Yao, Z. Pan, J. Zhai, G. Zhang, Z. Liu, and Y. Liu, Compos. Part A Appl. Sci. Manuf. **109**, 48 (2018).
[74]T. Hu, J. Juuti, H. Jantunen, and T. Vilkman, J. Eur. Ceram. Soc. **27**, 3997 (2007).
[75]A. Jain, A. K, J. Prashanth, A. K. Sharma, A. Jain, and P. N. Rashmi, Polym. Eng. Sci. **55**, 1589 (2015).
[76]Z. M. Dang, T. Zhou, S. H. Yao, J. K. Yuan, J. W. Zha, H. T. Song, J. Y. Li, Q. Chen, W. T. Yang, and J. Bai, Adv. Mater. **21**, 2077 (2009).
[77]H. Li, F. Liu, B. Fan, D. Ai, Z. Peng, and Q. Wang, Small Methods **2**, 1700399 (2018).
[78]W. Sun, X. Lu, J. Jiang, X. Zhang, P. Hu, M. Li, Y. Lin, C. W. Nan, and Y. Shen, J. Appl. Phys. **121**, 244101 (2017).
[79]D. Ai, H. Li, Y. Zhou, L. Ren, Z. Han, B. Yao, W. Zhou, L. Zhao, J. Xu, and Q. Wang, Adv. Energy Mater. **10**, 1903881 (2020).
[80]J. N. Coleman, U. Khan, and Y. K. Gun'ko, Adv. Mater. **18**, 689 (2006).
[81]H. Tang, Y. Lin, and H. A. Sodano, Adv. Energy Mater. **3**, 451 (2013).
[82]S. J. Zhou, C. Y. Ma, Y. Y. Meng, H. F. Su, Z. Zhu, S. L. Deng, and S. Y. Xie, Nanotechnology **23**, 055708 (2012).
[83]C. Zhi, Y. Bando, C. Tang, H. Kuwahara, and D. Golberg, Adv. Mater. **21**, 2889 (2009).
[84]X. Wang, A. Pakdel, J. Zhang, Q. Weng, T. Zhai, C. Zhi, D. Colberg, and Y. Bando, Nanoscale Res. Lett. **7**, 662 (2012).
[85]A. Esfandiari, H. Nazokdast, A. S. Rashidi, and M. E. Yazdanshenas, J. Appl. Sci. **8**, 545 (2008).
[86]F. Liu, Q. Li, Z. Li, Y. Liu, L. Dong, C. Xiong, and Q. Wang, Compos. Sci. Technol. **142**, 139 (2017).
[87]Q. Li, K. Han, M. R. Gadinski, G. Zhang, and Q. Wang, Adv. Mater. **26**, 6244 (2014).
[88]Y. Xie, J. Wang, Y. Yu, W. Jiang, and Z. Zhang, Appl. Surf. Sci. **440**, 1150 (2018).
[89]D. Wang, T. Zhou, J. W. Zha, J. Zhao, C. Y. Shi, and Z. M. Dang, J. Mater. Chem. A **1**, 6162 (2013).
[90]F. Liu, Q. Li, Z. Li, L. Dong, C. Xiong, and Q. Wang, Compos. Part A Appl. Sci. Manuf. **109**, 597 (2018).
[91]H. Li, L. Ren, D. Ai, Z. Han, Y. Liu, B. Yao, and Q. Wang, InfoMat **2**, 389 (2020).
[92]S. Luo, J. Yu, S. Yu, R. Sun, L. Cao, W. H. Liao, and C. P. Wong, Adv. Energy Mater. **9**, 1803204 (2019).
[93]Y. Li, Y. Zhou, Y. Zhu, S. Cheng, C. Yuan, J. Hu, J. He, and Q. Li, J. Mater. Chem. A **8**, 6576 (2020).
[94]H. Li, D. Ai, L. Ren, B. Yao, Z. Han, Z. Shen, J. Wang, L. Q. Chen, and Q. Wang, Adv. Mater. **31**, 1900875 (2019).
[95]M. Mackey, D. E. Schuele, L. Zhu, L. Flandin, M. A. Wolak, J. S. Shirk, A. Hiltner, and E. Baer, Macromolecules **45**, 1954 (2012).
[96]X. Zhang, J. Jiang, Z. Shen, Z. Dan, M. Li, Y. Lin, C. W. Nan, L. Q. Chen, and Y. Shen, Adv. Mater. **30**, 1707269 (2018).
[97]J. Jiang, Z. Shen, X. Cai, J. Qian, Z. Dan, Y. Lin, B. Liu, C. W. Nan, L. Q. Chen, and Y. Shen, Adv. Energy Mater. **9**, 1803411 (2019).
[98]Y. Wang, J. Chen, Y. Li, Y. Niu, Q. Wang, and H. Wang, J. Mater. Chem. A **7**, 2965 (2019).
[99]Y. Zhu, Y. Zhu, X. Huang, J. Chen, Q. Li, J. He, and P. Jiang, Adv. Energy Mater. **9**, 1901826 (2019).
[100]Y. Wang, L. Wang, Q. Yuan, J. Chen, Y. Niu, X. Xu, Y. Cheng, B. Yao, Q. Wang, and H. Wang, Nano Energy **44**, 364 (2018).
[101]Q. Li, F. Liu, T. Yang, M. R. Gadinski, G. Zhang, L. Q. Chen, and Q. Wang, Proc. Natl. Acad. Sci. U.S.A. **113**, 9995 (2016).
[102]A. Azizi, M. R. Gadinski, Q. Li, M. A. AlSaud, J. Wang, Y. Wang, B. Wang, F. Liu, L. Q. Chen, N. Alem, and Q. Wang, Adv. Mater. **29**, 1701864 (2017).
[103]Z. Cui, Z. Cao, R. Ma, A. V. Dobrynin, and D. H. Adamson, ACS Appl. Mater. Interfaces **7**, 16913 (2015).
[104]G. Liu, T. Zhang, Y. Feng, Y. Zhang, C. Zhang, Y. Zhang, X. Wang, Q. Chi, Q. Chen, and Q. Lei, Chem. Eng. J. **389**, 124443 (2020).
[105]S. Cheng, Y. Zhou, J. Hu, J. He, and Q. Li, IEEE Trans. Dielectr. Electr. Insul. **27**, 498 (2020).
[106]X. Huang and P. Jiang, Adv. Mater. **27**, 546 (2015).
[107]H. Luo, S. Chen, L. Liu, X. Zhou, C. Ma, W. Liu, and D. Zhang, ACS Sustain. Chem. Eng. **7**, 3145 (2019).
[108]X. Zhang, B. W. Li, L. Dong, H. Liu, W. Chen, Y. Shen, and C. W. Nan, Adv. Mater. Interfaces **5**, 1800096 (2018).
[109]H. Luo, X. Zhou, C. Ellingford, Y. Zhang, S. Chen, K. Zhou, D. Zhang, C. R. Bowen, and C. Wan, Chem. Soc. Rev. **48**, 4424 (2019).
[110]Y. Zhou, Y. Yuan, S. Wang, Y. Zhu, S. Cheng, X. Yang, Y. Yang, J. Hu, J. He, and Q. Li, Energy Stor. Mater. **28**, 255 (2020).
[111]Y. Thakur, T. Zhang, C. Iacob, T. Yang, J. Bernholc, L. Q. Chen, J. Runt, and Q. M. Zhang, Nanoscale **9**, 10992 (2017).
[112]T. Zhang, X. Chen, Y. Thakur, B. Lu, Q. Zhang, J. Runt, and Q. M. Zhang, Sci. Adv. **6**, eaax6622 (2020).